Amylopectin Wrapped Graphene Oxide/Sulfur for Improved Cyclability of Lithium–Sulfur Battery

Weidong Zhou,[†] Hao Chen,[†] Yingchao Yu, Deli Wang, Zhiming Cui, Francis J. DiSalvo, and Héctor D. Abruña*

Baker Laboratory, Department of Chemistry and Chemical Biology, Cornell University, Ithaca, New York, 14853, United States. [†]These authors contributed equally (W.Z., H.C.).

ABSTRACT An amylopectin wrapped graphene oxide-sulfur composite was prepared to construct a 3-dimensionally cross-linked structure through the interaction between amylopectin and graphene oxide, for stabilizing lithium sulfur batteries. With the help of this cross-linked structure, the sulfur particles could be confined much better among the layers of graphene oxide and exhibited significantly improved cyclability, compared with the unwrapped graphene oxide-sulfur composite. The effect of the electrode mass loading on electrochemical performance was investigated as well. In the lower sulfur mass loading cells, such as 2 mg cm^{-2}, both the capacity and the efficiency were obviously better than those of the higher sulfur mass loading cells, such as 6 mg cm^{-2}.

KEYWORDS: Li–S · battery · cathode · amylopectin · graphene oxide

There is currently a great deal of interest in the development of high energy and power density and long life rechargeable batteries for transportation and grid applications. Much attention has been focused on lithium ion batteries (LIBs) due to their potentially high energy density and low cost. The typical cathode materials most widely used in commercial LIBs are $LiCoO_2$, $LiMn_2O_4$, and $LiFePO_4$. However, they are limited by their relatively high cost, as in the case of cobalt, and low energy density.[1−3] Although the theoretical capacities can reach 300 mAh g^{-1}, the maximum practical capacities obtained are typically less than 200 mAh g^{-1}. Compared with the relatively large capacity of current anodes, the use of cathodes based on transition metals puts a theoretical limit on LIB systems for large scale energy storage. Lithium–sulfur (Li/S) batteries, represent one of the most promising candidates for next generation LIBs owing to their high theoretical capacity of 1673 mAh g^{-1}, which is about five times that of current commercial cathodes.[4] Although the voltage of Li/S cells is around 2.1–2.3 V (relative to Li/Li^+), the very high capacity and low cost overcome this limitation. However, despite their attractive properties, Li/S batteries suffer from poor cyclability, which is mainly attributed to the dissolution of intermediate lithium polysulfide products Li_2S_n ($4 \leq n \leq 8$), volumetric expansion and the poor conductivity of sulfur and polysulfide species.[5−7] In order to address these challenges, various methods have been reported including the use of mesoporous carbon,[8−16] graphene oxide,[17,18] carbon nanotube,[19−21] and sulfur-coating polymer composites.[22−24] Among these, mesoporous carbon-based materials with a pore size of less than 5 nm show attractive performance due to their obvious advantages on high conductivity and large surface area. However, the preparation of mesoporous carbons usually involves the use of highly toxic hydrofluoric acid to remove the hard template.[8−16] And from the impregnation of sulfur into mesoporous carbons, if the sulfur could diffuse into the small pores of the mesoporous carbons, the sulfur could also diffuse out during long cycling, considering the fact that the sulfur can still be accessed by electrolyte for long terms. Although the weak interactions between sulfur and mesopores could alleviate the dissolution of polysulfides in a short-term, the polysulfides should still be dissolved and diffuse out eventually. This is likely the reason why extended cycle life (>100 cycles)

* Address correspondence to hda1@cornell.edu.

Received for review June 25, 2013 and accepted September 5, 2013.

Published online September 05, 2013
10.1021/nn403237b

tests with stable capacity retention and high Coulombic efficiency were rarely reported for this type of Li/S composites. In addition, the mesoporous carbon/sulfur composites were constructed through the diffusion of sulfur vapor or liquid sulfur into the nanopores of mesoporous carbon, which limits the sulfur loading in the electrode composites. Another innegligible phenomenon in Li/S batteries is that polyvinylidene fluoride (PVDF) dissolved in *N*-methyl-2-pyrrolidone (NMP) was generally employed as the binder. However, NMP could dissolve the sulfur, which will destroy the preconstructed nanostrucutures and the evaporation of NMP under vacuum could also cause related environmental problems.[25] To overcome these limitations, more feasible methods need to be explored to immobilize the lithium polysulfides at lower cost and can be easily scaled up in industry.

According to the recent studies, graphene-oxide (GO)-doped sulfur in Li/S electrode composite show promising improvement for the cycling stability of the corresponding batteries.[17,18] GO consists of a basal plane decorated mostly with epoxide and hydroxyl groups, in addition to carbonyl and carboxyl groups, which are located at the edges.[26−29] These groups in GO play important role for immobilizing the otherwise free lithium polysulfides.[17] However, the stable charge−discharge process of pure GO-coated sulfur composite can only be observed at initial 30 cycles, followed by an obvious capacity fading. When a PEG surfactant-coated sulfur was wrapped with GO, the capacity dropped from initial 1000 to 550 mAh g^{-1} after 20 cycles.[18] This capacity fading is probably because the superficial sulfur cannot be fully trapped and the open channels among the GO layers provide large space for polysulfides to escape. To further immobilize the polysulfides, a soft polymer should be employed to wrap the GO/S composite and construct a 3-dimensional network for better immobilizing the polysulfide species and accommodating the volumetric expansion during cycling. The polymer had better interact with the marginal hydroxyl and carboxyl group of the GO for binding the margins of adjacent GO layers to avoid the polysulfide diffusing out of the GO layers. In the meantime, it should be both insoluble and nonredox active in the LIBs potential window.

With this consideration in mind, a natural polymer, amylopectin was pitched on here because sufficient hydroxyl units of amylopectin will interact with the hydroxyl group of GO through hydrogen bonding interaction to form cross-linked 3-dimensional structure, helping to bind the GO layers and accommodate the volumetric expansion, and it is environmentally benign.[30−33] Recently, gelatin and β-cyclodextrin were tested as aqueous binders of the Li−S batteries for the immobilization of polysulfides, which gave improved cyclability in the initial 50 cycles.[34,35] Water-soluble brown algae was also harnessed as a binder to build silicon nanopowder-based lithium ion batteries and gave improved performance.[36] Herein, the reasonable combination of amylopectin wrapped GO-sulfur as electrode composite for improvement of sulfur electrode stability was investigated. As expected, with the assistance of this structure, the cycling stability of the sulfur electrode was enhanced significantly compared with the unwrapped GO-sulfur composite. This cross-linked build-up, constructed through the intermolecular interactions, provides new opportunities to mitigate the diffusion of lithium polysulfide species and improves the cycling stability of Li/S batteries.

RESULTS AND DISCUSSION

A control sample of amylopectin doped sulfur without GO (but contained carbon black) was first prepared to test the electrochemical properties. Sulfur and carbon black were first heated to 155 °C for 12 h to obtain a homogeneously mixed material. The mixture was dispersed in an aqueous amylopectin solution under sonication and excess ethanol was then added slowly to yield the black precipitation of amylopectin coated sulfur (S-Amy) composite. According to the thermogravimetric analysis (TGA) curve of the obtained black powder, in Figure S1 of the Supporting Information (SI), around 56% sulfur and 14% amylopectin were contained in the composite. It was then ground in the presence of 5% polytetrafluoroethylene (PTFE) to lower the stiffness of amylopectin, giving the electrode films with an average sulfur mass loading of 4.0 mg cm^{-2}. Coin cells were fabricated to test the electrochemical performance of the S-Amy composite using lithium foil as the anode and 1.0 M lithium bis-trifluoromethanesulfonylimide (LiTFSI) in a mixed solvent of 1,3-dioxolane and 1,2-dimethoxyethane (1:1, v/v) as the electrolyte.

A cyclic voltammetry (CV) of a Li/S cell with the S-Amy cathode was obtained at a scan rate of 0.05 mV s^{-1} and was shown in Figure S2 of the SI. Two well-defined reduction peaks at 2.35 and 2.08 V were observed, which could be assigned to the multistep reduction mechanism of elemental sulfur, as reported previously.[8−24] The reduction peak centered around 2.35 V is generally attributed to the reduction of the S_8 ring and the formation of S_8^{2-}. The reduction peak at 2.08 V is associated with further reduction of the higher polysulfide species (Li_2S_n, $4 < n < 8$) to the lower polysulfide species (Li_2S_n, $n \leq 2$). The broad oxidation peak around 2.3−2.5 V is associated with the oxidation of polysulfides to the neutral elemental S_8.[9]

Figure 1a depicted the 1st and 40th discharge/charge profiles of the S-Amy electrode at a rate of C/8 in a rechargeable lithium cell. Two flat discharge plateaus located at 2.35 and 2.08 V were clearly observed, in good agreement with the CV results. As shown in Figure 1b, the S-Amy electrode showed an initial discharge capacity of 825 mAh g^{-1} followed by a gradual decrease during subsequent cycles. Compared

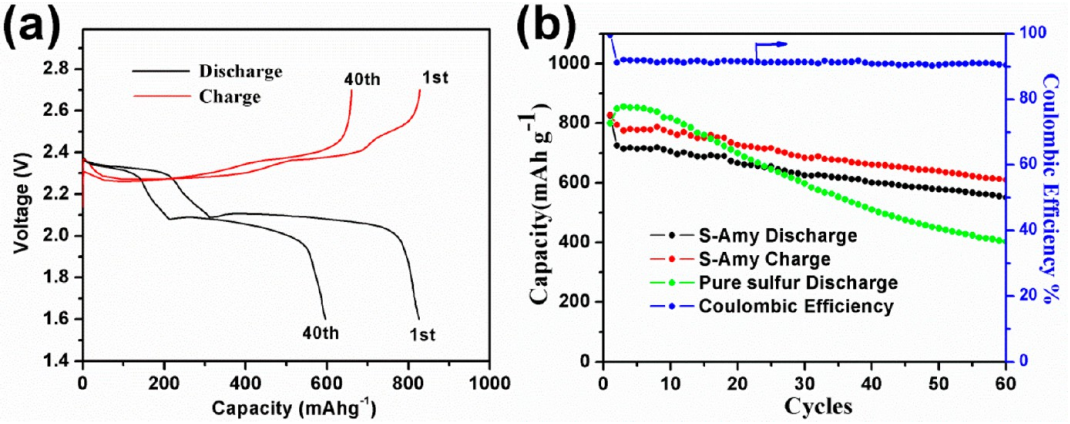

Figure 1. (a) Charge/discharge profiles and (b) charge/discharge capacities *vs* cycle number for S-Amy cathode at a rate of C/8. 1C corresponds to a current density of 1600 mA/g and the capacity values are calculated based on the mass of sulfur.

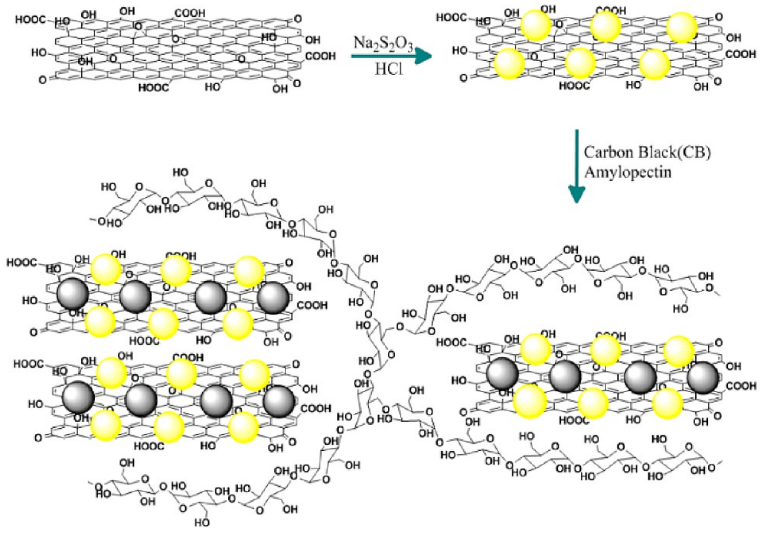

Scheme 1. Schematic Two-Step Synthesis Route for a GO-S-Amy Composite, with Yellow Balls Representing Sulfur and Black Balls Representing Carbon Black

with the cycling performance of the pure sulfur electrode, although the pure sulfur cathode exhibited a higher capacity in initial 25 cycles, it exhibited a much faster capacity fade especially after 30 cycles. The relatively slow capacity fading of S-Amy electrode indicates that the addition of amylopectin can alleviate, at least in part, the diffusion of the lithium polysulfides into the electrolyte and therefore suggests that the amylopectin could be adopted as an additive for Li/S batteries.[34−36] On the other hand, the Coulombic efficiency of the S-Amy electrode stabilized at a little over than 90% and the capacity obviously still faded, which indicates there are still some polysulfide dissolution and shuttling of the polysulfide species.[37]

The amylopectin wrapped graphene oxide-sulfur (GO-S-Amy) composite was subsequently prepared through a quite sample dissolution−precipitation method. In our approach (Scheme 1), a mildly oxidized Hummers GO was employed in the electrode composite.[18,29] The GO was first dispersed in the solution of sodium thiosulfate under sonication to form a homogeneous suspension. Sulfur particles could then be synthesized and precipitated homogeneously among GO layers by reacting sodium thiosulfate with hydrochloric acid. As shown in the TGA curve of Figure S3 in the SI, around 72 wt % of sulfur was incorporated in the GO-S composite. The as prepared GO-S and carbon black were dispersed in an aqueous solution of amylopectin through sonication. Excess ethanol was then slowly added to give the GO-S-Amy floccus precipitation, which was employed to make the electrode film after drying in vacuum. According to the TGA results of Figure S4 in the SI, the final sulfur content in the whole electrode was around 52% accounting 5% PTFE binder added during the preparation of the electrode film. This approach is much simpler and economical when compared with the widely used procedure of long time or repeated sublimation for infusion of elemental sulfur into porous carbons. Also, such a process is environmentally benign and highly reproducible, and can be straightforward to scale up in industry.

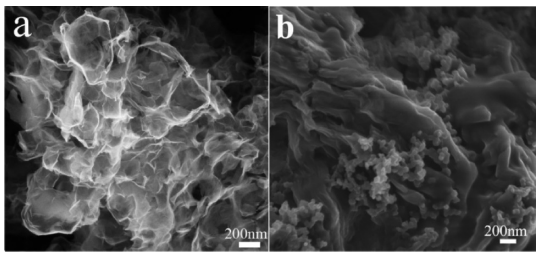

Figure 2. SEM images of GO (a) and GO-S-Amy (b) composite.

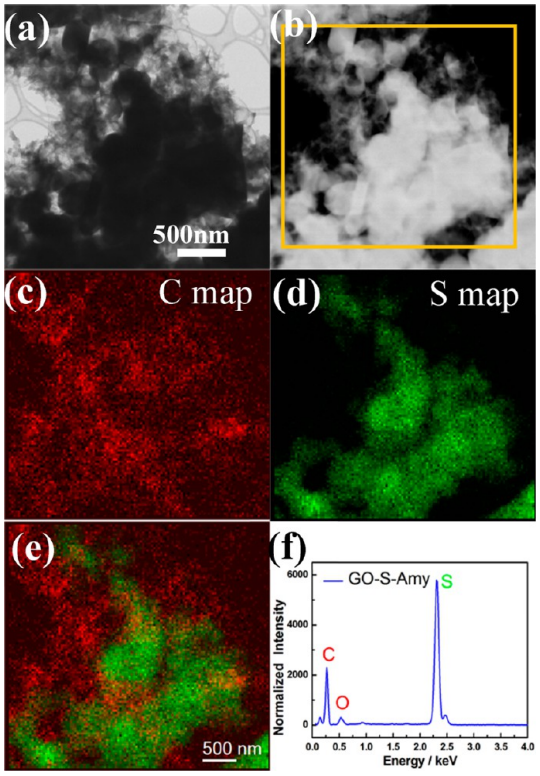

Figure 3. STEM images of GO-S-Amy in bright field (a) and dark field (b). Elemental mapping of the region shown in the yellow square of (b) for carbon (c) and sulfur (d), along with (e) an overlay of those two maps. (f) EDX spectrum of GO-S-Amy composite.

Figure 2 exhibits the scanning electron microscopy (SEM) images of the GO and GO-S-Amy composite. Compared with the well-defined flake structure of GO, amorphous and aggregated nanosheets with carbon black particles on the surface were observed for the GO-S-Amy composite, which could be attributed to the interaction between amylopectin and GO. In the scanning transmission electron microscopy (STEM) images of GO-S-Amy composite, sulfur particles with a diameter of around 500 nm could be clearly observed, as shown in Figure 3a,b. Elemental maps of sulfur and carbon (Figure 3) confirmed that the bright particles in Figure 3b were sulfur particles, along with overlaying carbon signals from GO sheets. Associated with the SEM image of Figure 2b, the sulfur particles should have been confined among the GO layers, because there was no sulfur particle could be observed on the

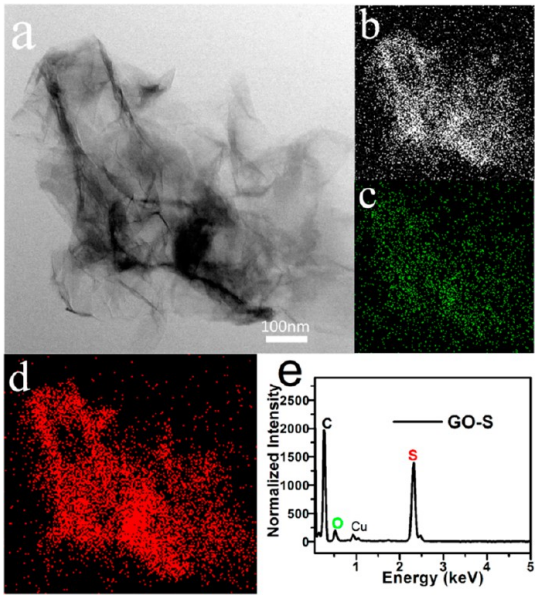

Figure 4. STEM bright field image of the GO-S composite (a) and the corresponding elemental mapping for carbon (b), oxygen (c), and sulfur (d). (e) EDX spectrum of GO-S composite.

surface from the SEM image. Energy-dispersive X-ray (EDX) microanalysis exhibited strong sulfur peak, which is around three times of carbon, as shown in Figure 3f. The relative content of sulfur in GO-S-Amy should be higher considering that the carbon contribution of amylopectin and the carbon film on the STEM grid was also included in the EDX intensity of carbon. In the case of unwrapped GO-S, the sulfur particles could not be observed in the STEM images, as shown in Figure 4, which can be attributed to the high vacuum of STEM and high vapor pressure of the sulfur.[38,39] Although elemental sulfur could still be detected in the sulfur map, the EDX intensity of sulfur is obviously smaller compared with the carbon, which suggests most of the sulfur in GO-S was evaporated in the high vacuum of STEM. These features, from one side, verified that the amylopectin wrapped GO effectively confined the sulfur among GO layers.

The obtained dry GO-S-Amy composite was employed to make the electrode films with several typical sulfur mass loadings of 2.0 mg cm^{-2}, 4.0 and 6.0 mg cm^{-2} through control the thickness of electrode films. Figure 5 shows the CV and cycling performance of coin cells using GO-S-Amy as the cathode with a suffer loading of 4.0 mg cm^{-2}. Two well-defined reduction peaks centered around 2.3 and 2.03 V were clearly observed, similar to the CV of the S-Amy electrode described above. During the initial 10 cycles, the redox curves become sharper gradually, suggesting the reversibility actually improved with cycling. As illustrated in Figure 5b, the GO-S-Amy electrodes showed initial capacities of 817, 650, and 596 mAh g^{-1} under different C rates of C/8, 5C/16, and C/2, respectively. Although there was an

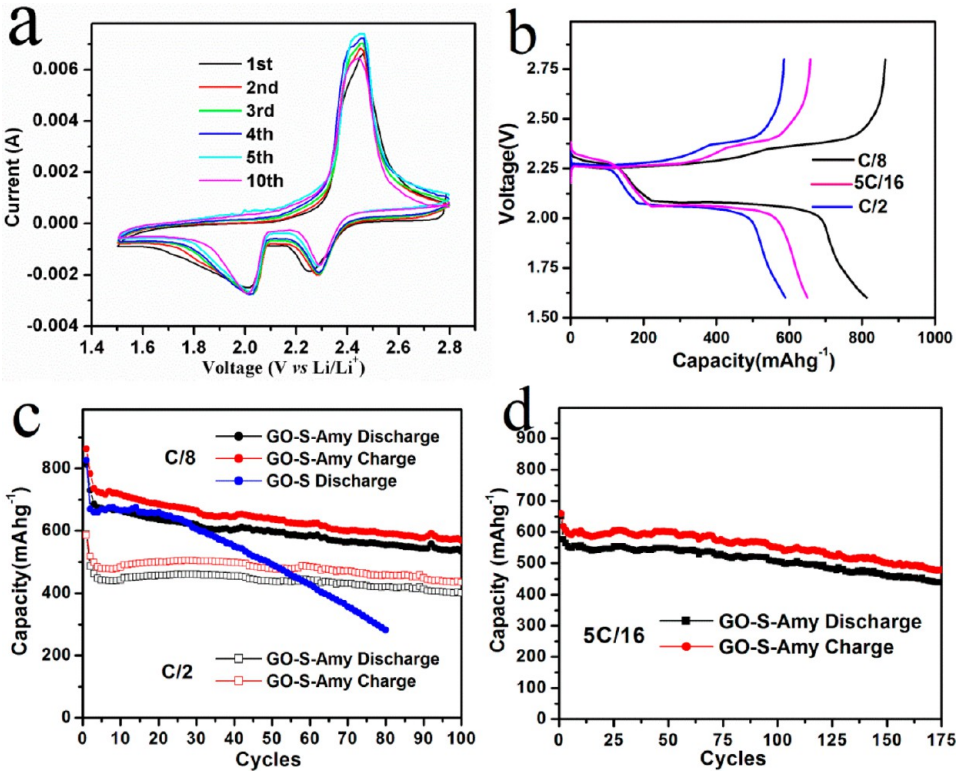

Figure 5. (a) Typical CV of GO-S-Amy cathode at a sweep rate of 0.1 mV s^{-1}; (b) First cycle charge/discharge profiles for the GO-S-Amy cathodes at current densities of C/8, 5C/16, and C/2; (c, d) Charge/discharge capacities *vs* cycle numbers of GO-S and GO-S-Amy at different current densities.

initial drop, the capacity stabilized after about five cycles at both low and high current densities, as observed in Figure 5c. Afterward, there was a much more gradual decrease in capacity. A control sample of GO-S without amylopectin coating exhibited a stable cyclability during the first 25 cycles, followed by a significant capacity fading. Relative to the unwrapped GO-S electrode, the GO-S-Amy electrode exhibited much improved capacity retention with long cycling, which was ascribed to the cross-linked structures of amylopectin-wrapped GO and polysulfides. After a long-term cycling of 175 cycles, a discharge capacity of 441 mAh g^{-1} was obtained at 5C/16, which corresponded to a 68% capacity retention ratio, as shown in Figure 5d. At the higher current density of C/2, much more stable cycling performance was observed, with a stable capacity around 430 mAh g^{-1}, which did not decay significantly after 100 cycles. The relatively better cycling performance at C/2 can be attributed to the weaker shuttle effect at higher current density.[18] The improved cycling stability verifies the fact that the amylopectin-wrapped GO-S structure can help to immobilize the polysulfides and reduce the capacity fading, which was in agreement with the successful confinement of sulfur under high vacuum of STEM. The branched amylopectin could wrap and bind GO layers effectively through its cross-linked 3-dimension structure and supramolecular interaction, which closes the open channels among GO layers and minimizes the diffusion of the polysulfides. As a result, electrodes employing the amylopectin wrapped GO-sulfur exhibited better cycling stability.

Figure 6 shows the charge−discharge profiles and cycling performance of the GO-S-Amy composite electrodes with different sulfur loadings of 2 and 6 mg cm^{-2} at C/8. Obviously, the lower suffer loading of 2 mg cm^{-2} GO-S-Amy cathode delivered higher discharge capacity and efficiency in this condition. From the Figure S6 of SI, the Coulombic efficiencies of the electrode with different sulfur loadings of 2, 4, and 6 mg cm^{-2} at C/8 were around 98, 94, and 91%, respectively. Here, lower capacity at higher suffer loading can be attributed to the poorer ionic transportation and contact in thicker electrode film. We should point out that, although this composite showed better cycling stability compared with the pure sulfur and unwrapped GO-S, slow capacity degradation could still be observed. Besides, the efficiency was just around 98% even in low sulfer loading of 2 mg cm^{-2}, which indicates that the dissolution of polysulfides and the subsequent shuttling effect are still not completely absent in this condition. But the low cost of materials and the easy scaled up preparation process give the competitive advantage for this structure.

To further investigate the structure of the GO-S-Amy composite during the long cycling, a cell was opened after the 50th full discharge in cell and the electrode was peeled off from the current collector and redispersed in THF under sonication. As shown in the STEM

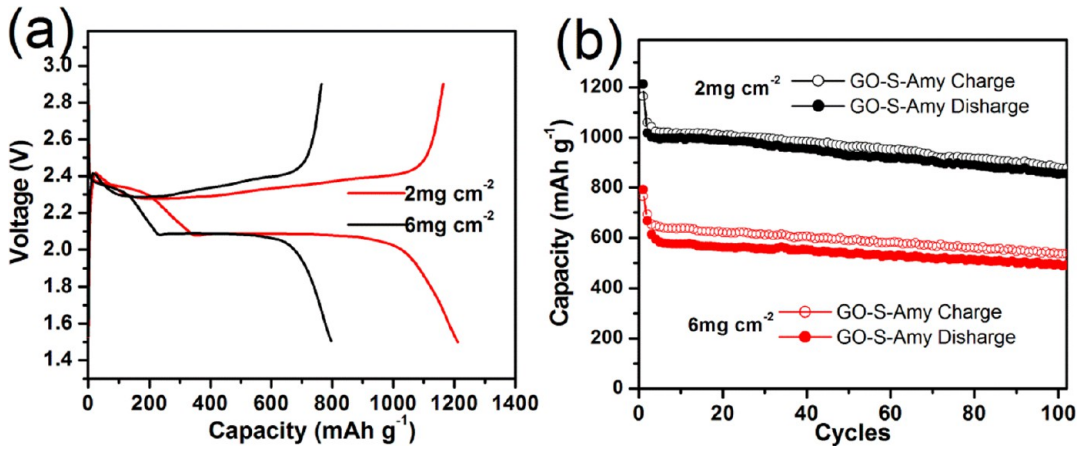

Figure 6. (a) First cycle charge/discharge profiles for the GO-S-Amy cathodes with the sulfur loadings of 2 and 6 mg cm^{-2} at C/8; (b) Charge/discharge capacities *vs* cycle numbers of GO-S-Amy at different sulfur loadings.

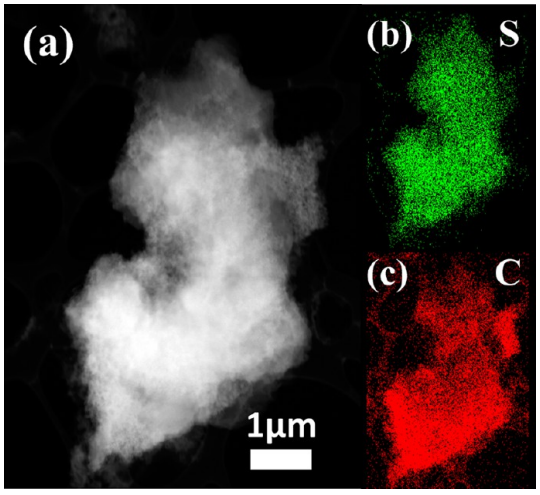

Figure 7. STEM dark field image of GO-S-Amy composite after the 50th discharge in the cell (a) and corresponding elemental mapping for sulfur (b) and carbon (c).

images and EDX mapping of Figure 7, the sulfur particles were disappeared and the elemental sulfur dispersed homogeneously among the GO layers, owing to the precipitation of a thin layer of discharge products (Li_2S_2 and Li_2S). EDX spectrum of GO-S-Amy composite after the 50th discharge exhibited strong signal of sulfur, as shown in the Figure S7 of SI. It is also noticeable that the architecture of GO-S was still maintained after running 50 cycles, which indicates the stability of this structure. The Fourier transform infrared spectroscopy (FTIR) spectra of the 50th discharged cathode exhibited obvious peaks at 1580, 1426, and 850 cm^{-1}, as shown in the Figure S8 of the SI, suggesting the formation of S−Li or O−Li.[38,40] The summit of broad band between 3600 and 2600 cm^{-1} resulting from the O−H groups of GO-S-Amy (after the 50th discharge) shifted toward short wavenumber compared with that of GO-S-Amy, which indicates the presence of the hydrogen bonds in discharged GO-S-Amy composite. Meanwhile, an obvious shoulder at 2535 cm^{-1} could be ascribed to the S−H stretching vibration, which suggested the presence of the balance between O−H and S−H.[38,40] These observations, including the STEM and FTIR, suggest that the GO-S-Amy composite forms a stable cross-linked structure through the supramolecular interactions, which can accommodate the charge/discharge reactions and preserve the structure in long cycling.

CONCLUSIONS

In summary, a natural polymer, amylopectin-wrapped GO-S nanocomposite has been prepared and investigated for immobilizing the lithium polysulfides in the cathode of Li/S cells. With the help of this 3-dimensionally cross-linked structure, the Li/S battery exhibited much improved cycling stability and Columbic efficiency compared with the conventional sulfur electrodes and unwrapped composite. From the comparison of STEM images and EDX data, the branched amylopectin wrapped GO-S successfully confined the sulfur particles among the GO layers, which helps to tether the polysulfides during the charge/discharge processes. Different sulfur loading electrodes were tested and compared as well; a lower sulfur loading electrode showed better capacity and efficiency relative to the higher sulfur loading electrode. While slight capacity fading presents in these and premier studies, we believe that these results provide reliable insights and novel concepts for future Li/S batteries.

EXPERIMENTAL METHODS

Preparation of S-Amy Composite Electrode. In a typical electrode making process of S-Amy, 50 mg sulfur and 25 mg carbon black were first heated at 155 °C for 12 h to obtain a homogeneous material. The mixture was dispersed in 100 mL of an aqueous solution of 15 mg amylopectin under sonication and heated at

80 °C for 1 h, and then 300 mL of ethanol was added slowly to yield the precipitation of an amylopectin-coated sulfur−carbon black composite. The above precipitation and 5% polytetrafluoroethylene (PTFE) were ground well in a mortar with the addition of isopropanol and then were roll-pressed to produce an electrode film, which was heated at 50 °C for 12 h under vacuum before using to make the coin cell. The coin cells were fabricated in an argon-filled glovebox using lithium metal as the counter electrode and a microporous polyethylene separator. The control experiment of pure sulfur coin cell was also fabricated according to the same procedure, except that the cathode composite was made from 50% elemental sulfur, 40% carbon black, and 10% PTFE binder.

Synthesis of GO-S-Amy Composite. A total of 60 mg GO was well dispersed in 100 mL of water through a 1 h sonication to obtain a black homogeneous suspension. For sulfur particles synthesis, 2.0 g of $Na_2S_2O_3$ was first dissolved in 400 mL of 1% PVP aqueous solution. Then 6 mL of concentrated hydrochloric acid was added to the above solution, and the system was kept at room temperature for 40 min with magnetic stirring to get a white gel solution of sulfur particles. The suspension of GO was then added into the sulfur gel solution under vigorous magnetic stirring. After 20 min, the product of GO-S was collected by centrifuge and further washed twice with water. A total of 10 mg amylopectin was suspended in 100 mL of water and then heated to 80 °C for 1 h to get a transparent solution. Freshly prepared 70 mg of GO-S and 15 mg carbon black were added to the above solution and stirred for 30 min under sonication for intensive mixing. The resulting suspension was poured into 300 mL of ethanol, filtered, and dried to get a black powder. The obtained powder and 5% PTFE were ground well in a mortar with the addition of isopropanol and then were roll-pressed to produce an electrode film, which was heated at 50 °C for 12 h under vacuum before using to fabricate the coin cell. The GO-S-Amy coin cell was fabricated according to a similar procedure as for the S-Amy coin cell.

Conflict of Interest: The authors declare no competing financial interest.

Supporting Information Available: More detailed material characterization data are included, such as the TGA curves, XRD data, FTIR data, EDX data, CV curves, and instrument parameters. This material is available free of charge *via* the Internet at http://pubs.acs.org.

Acknowledgment. This work was supported by the Department of Energy though Grant DE-FG02-87ER45298, by the Energy Materials Center at Cornell (EMC2), an Energy Frontier Research Center funded by the U.S. Department of Energy, Office of Basic Energy Sciences under Award Number DE-SC0001086. This work made use of the electron microscopy facility of the Cornell Center for Materials Research (CCMR) with support from the National Science Foundation Materials Research Science and Engineering Centers (MRSEC) program (DMR 1120296).

REFERENCES AND NOTES

1. Whittingham, M. S. Lithium Batteries and Cathode Materials. *Chem. Rev.* **2004**, *104*, 4271–4301.
2. Aricò, A. S.; Bruce, P.; Scrosati, B.; Tarascon, J.-M.; Schalkwijk, W. V. Nanostructured Materials for Advanced Energy Conversion and Storage Devices. *Nat. Mater.* **2005**, *4*, 366–377.
3. Guo, Y.; Hu, J.; Wan, L. Nanostructured Materials for Electrochemical Energy Conversion and Storage Devices. *Adv. Mater.* **2008**, *20*, 2878–2887.
4. Bruce, P. G.; Freunberger, S. A.; Hardwick, L. J.; Tarascon, J.-M. Li-O_2 and Li-S Batteries with High Energy Storage. *Nat. Mater.* **2012**, *11*, 19–29.
5. Mikhaylik, Y. V.; Kovalev, I.; Schock, R.; Kumaresan, K.; Xu, J.; Affinito, J. High Energy Rechargeable Li-S Cells for EV Application: Status, Remaining Problems and Solutions. *ECS Trans.* **2010**, *25*, 23–34.
6. Yamin, H.; Gorenshtein, A.; Penciner, J.; Sternberg, Y.; Peled, E. Lithium Sulfur Battery Oxidation/Reduction Mechanisms of Polysulfides in THF Solutions. *J. Electrochem. Soc.* **1988**, *135*, 1045–1048.
7. Peled, E.; Sternberg, Y.; Gorenshtein, A.; Lavi, Y. Lithium-Sulfur Battery: Evaluation of Dioxolane-Based Electrolytes. *J. Electrochem. Soc.* **1989**, *136*, 1621–1625.
8. Jayaprakash, N.; Shen, J.; Moganty, S. S.; Corona, A.; Archer, L. A. Porous Hollow Carbon@Sulfur Composites for High-Power Lithium-Sulfur Batteries. *Angew. Chem., Int. Ed.* **2011**, *50*, 5904–5908.
9. Liang, C.; Dudney, N. J.; Howe, J. Y. Hierarchically Structured Sulfur/Carbon Nanocomposite Material for High-Energy Lithium Battery. *Chem. Mater.* **2009**, *21*, 4724–4730.
10. Xiao, L.; Cao, Y.; Xiao, J.; Schwenzer, B.; Engelhard, M. H.; Saraf, L. V.; Nie, Z.; Exarhos, G. J.; Liu, J. A Soft Approach to Encapsulate Sulfur: Polyaniline Nanotubes for Lithium-Sulfur Batteries with Long Cycle Life. *Adv. Mater.* **2012**, *24*, 1176–1181.
11. Zhang, C.; Wu, H.; Yuan, C.; Guo, Z.; Lou, X. W. Confining Sulfur in Double-Shelled Hollow Carbon Spheres for Lithium-Sulfur Batteries. *Angew. Chem., Int. Ed.* **2012**, *51*, 9592–9595.
12. Ji, X.; Lee, K. T.; Nazar, L. F. A Highly Ordered Nanostructured Carbon-Sulphur Cathode for Lithium-Sulphur Batteries. *Nat. Mater.* **2009**, *8*, 500–506.
13. Yang, Y.; Yu, G.; Cha, J. J.; Wu, H.; Vosgueritchian, M.; Yao, Y.; Bao, Z.; Cui, Y. Improving the Performance of Lithium-Sulfur Batteries by Conductive Polymer Coating. *ACS Nano* **2011**, *5*, 9187–9193.
14. Ji, X.; Evers, S.; Black, R.; Nazar, L. F. Stabilizing Lithium-Sulphur Cathodes Using Polysulphide Reservoirs. *Nat. Commun.* **2011**, *2*, 325.
15. Schuster, J.; He, G.; Mandlmeier, B.; Yim, T.; Lee, K. T.; Bein, T.; Nazar, L. F. Spherical Ordered Mesoporous Carbon Nanoparticles with High Porosity for Lithium-Sulfur Batteries. *Angew. Chem., Int. Ed.* **2012**, *51*, 3591–3595.
16. Xin, S.; Gu, L.; Zhao, N.; Yin, Y.; Zhou, L.; Guo, Y.; Wan, L. Smaller Sulfur Molecules Promise Better Lithium-Sulfur Batteries. *J. Am. Chem. Soc.* **2012**, *134*, 18510–18513.
17. Ji, L.; Rao, M.; Zheng, H.; Zhang, L.; Li, Y.; Duan, W.; Guo, J.; Cairns, E. J.; Zhang, Y. Graphene Oxide as a Sulfur Immobilizer in High Performance Lithium/Sulfur Cells. *J. Am. Chem. Soc.* **2011**, *133*, 18522–18525.
18. Wang, H.; Yang, Y.; Liang, Y.; Robinson, J. T.; Li, Y.; Jackson, A.; Cui, Y.; Dai, H. Graphene-Wrapped Sulfur Particles as a Rechargeable Lithium-Sulfur Battery Cathode Material with High Capacity and Cycling Stability. *Nano Lett.* **2011**, *11*, 2644–2647.
19. Han, S.-C.; Song, M.-S.; Lee, H.; Kim, H.-S.; Ahn, H.-J.; Lee, J.-Y. Effect of Multiwalled Carbon Nanotubes on Electrochemical Properties of Lithium/Sulfur Rechargeable Batteries. *J. Electrochem. Soc.* **2003**, *150*, A889–A893.
20. Yin, L.; Wang, J.; Yang, J.; Nuli, Y. A Novel Pyrolyzed Polyacrylonitrile-sulfur@MWCNT Composite Cathode Material for High-Rate Rechargeable Lithium/Sulfur Batteries. *J. Mater. Chem.* **2011**, *21*, 6807–6810.
21. Wu, F.; Chen, J.; Li, L.; Zhao, T.; Chen, R. Improvement of Rate and Cycle Performence by Rapid Polyaniline Coating of a MWCNT/Sulfur Cathode. *J. Phys. Chem. C* **2011**, *115*, 24411–24417.
22. Wu, F.; Chen, J.; Chen, R.; Wu, S.; Li, L.; Chen, S.; Zhao, T. Sulfur/Polythiophene with a Core/Shell Structure: Synthesis and Electrochemical Properties of the Cathode for Rechargeable Lithium Batteries. *J. Phys. Chem. C* **2011**, *115*, 6057–6063.
23. Manthiram, A.; Fu, Y.; Su, Y.-S. Challenges and Prospects of Lithium-Sulfur Batteries. *Acc. Chem. Res.* **2013**, *46*, 1125–1134.
24. Seh, Z. W.; Li, W.; Cha, J. J.; Zheng, G.; Yang, Y.; McDowell, M. T.; Hsu, P.-C.; Cui, Y. Sulphur-TiO_2 Yolk-Shell Nanoarchitecture with Internal Void Space for Long-cycle Lithium-Sulphur Batteries. *Nat. Commun.* **2013**, *4*, 1331.
25. Schneider, H.; Garsuch, A.; Panchenko, A.; Gronwald, O.; Janssen, N.; Novák, P. Influence of Different Electrode Compositions and Binder Materials on the Performance of Lithium-Sulfur Batteries. *J. Power Sources* **2012**, *205*, 420–425.

26. Stankovich, S.; Dikin, D. A.; Piner, R. D.; Kohlhaas, K. A.; Kleinhammes, A.; Jia, Y.; Wu, Y.; Nguyen, S. T.; Ruoff, R. S. Synthesis of Graphene-Based Nanosheets *via* Chemical Reduction of Exfoliated Graphite Oxide. *Carbon* **2007**, *45*, 1558–1565.
27. Szabó, T.; Berkesi, O.; Dékány, I. DRIFT Study of Deuterium-Exchanged Graphite Oxide. *Carbon* **2005**, *43*, 3186–3189.
28. Lerf, A.; He, H.; Forster, M.; Klinowski, J. Structure of Graphite Oxide Revisited. *J. Phys. Chem. B* **1998**, *102*, 4477–4482.
29. Hummers, W. S.; Offeman, R. E. Preparation of Graphitic Oxide. *J. Am. Chem. Soc.* **1958**, *80*, 1339–1339.
30. Lawrence, D. S.; Jiang, T.; Levett, M. Self-Assembling Supramolecular Complexes. *Chem. Rev.* **1995**, *95*, 2229–2260.
31. Brunsveld, L.; Folmer, B. J. B.; Meijer, E. W.; Sijbesma, R. P. Supramolecular Polymers. *Chem. Rev.* **2001**, *101*, 4071–4098.
32. Amendola, V.; Esteban-Gómez, D.; Fabbrizzi, L.; Licchelli, M. What Anions Do to N-H-Containing Receptors. *Acc. Chem. Res.* **2006**, *39*, 343–353.
33. Beletskaya, I.; Tyurin, V. S.; Tsivadze, A. Y.; Guilard, R.; Stern, C. Supramolecular Chemistry of Metalloporphyrins. *Chem. Rev.* **2009**, *109*, 1659–1713.
34. Wang, J.; Yao, Z.; Monroe, C. W.; Yang, J.; Nuli, Y. Carbonyl-β-cyclodextrin as a Novel Binder for Sulfur Composite Cathodes in Rechargeable Lithium Batteries. *Adv. Funct. Mater.* **2013**, *23*, 1194–1201.
35. Huang, Y.; Sun, J.; Wang, W.; Wang, Y.; Yu, Z.; Zhang, H.; Wang, A.; Yuan, K. Discharge Process of the Sulfur Cathode with a Gelatin Binder. *J. Electrochem. Soc.* **2008**, *155*, A764–A767.
36. Kovalenko, I.; Zdyrko, B.; Magasinski, A.; Hertzberg, B.; Milicev, Z.; Burtovyy, R.; Luzinov, I.; Yushin, G. A Major Constituent of Brown Algae for Use in High-Capacity Li-Ion Batteries. *Science* **2011**, *334*, 75–79.
37. Mikhaylik, Y. V.; Akridge, J. R. Polysulfide Shuttle Study in the Li/S Battery System. *J. Electrochem. Soc.* **2004**, *151*, A1969–A1976.
38. Aurbach, D.; Pollak, E.; Elazari, R.; Salitra, G.; Kelley, C. S.; Affinito, J. On the Surface Chemical Aspects of Very High Energy Density, Rechargeable Li-Sulfur Batteries. *J. Electrochem. Soc.* **2009**, *156*, A694–A702.
39. Ferreira, A. G. M.; Lobo, L. Q. The Low-Pressure Phase Diagram of Sulfur. *J. Chem. Thermodyn.* **2011**, *43*, 95–104.
40. Diao, Y.; Xie, K.; Xiong, S.; Hong, X. Insights into Li-S Battery Cathode Capacity Fading Mechanisms: Irreversible Oxidation of Active Mass during Cycling. *J. Electrochem. Soc.* **2012**, *159*, A1816–A1821.